

University of Wollongong

Research Online

Faculty of Engineering and Information
Sciences - Papers: Part A

Faculty of Engineering and Information
Sciences

2013

Modeling and experimental investigation of rotational resistance of a spiral-type robotic capsule inside a real intestine

Hao Zhou

University of Wollongong, hz467@uowmail.edu.au

Gursel Alici

University of Wollongong, gursel@uow.edu.au

Trung Duc Than

University of Wollongong, dtt581@uowmail.edu.au

Weihua Li

University of Wollongong, weihuali@uow.edu.au

Follow this and additional works at: <https://ro.uow.edu.au/eispapers>



Part of the [Engineering Commons](#), and the [Science and Technology Studies Commons](#)

Recommended Citation

Zhou, Hao; Alici, Gursel; Than, Trung Duc; and Li, Weihua, "Modeling and experimental investigation of rotational resistance of a spiral-type robotic capsule inside a real intestine" (2013). *Faculty of Engineering and Information Sciences - Papers: Part A*. 1590.

<https://ro.uow.edu.au/eispapers/1590>

Research Online is the open access institutional repository for the University of Wollongong. For further information contact the UOW Library: research-pubs@uow.edu.au

Modeling and experimental investigation of rotational resistance of a spiral-type robotic capsule inside a real intestine

Abstract

In this study, the rotational resistance of a spiral-type capsule rotating inside a small intestine is investigated by in vitro experiments and analytical modeling, on which a limited literature is available. The results presented exhibit viscoelastic nature of the intestinal tissue. The significance of various spiral structures and rotating speeds is quantitatively evaluated from the propulsion point of view. Also, an analytical torque model is proposed and subsequently validated. The close match between the experimental results and numerical results from the model shows that the model is reasonably accurate to estimate the rotational resistance torque of the small intestine. Both the experimental and modeling works provide a useful guide to determine the torque required for a spiral-type endoscopic capsule operating in a 'really' small intestine. Therefore, the proposed torque model can be used in the design and optimization of in-body robotic systems, which can remotely be articulated using magnetic actuation.

Keywords

rotational, resistance, spiral, modeling, type, experimental, robotic, capsule, inside, real, intestine, investigation

Disciplines

Engineering | Science and Technology Studies

Publication Details

Zhou, H., Alici, G., Than, T. Duc. & Li, W. (2013). Modeling and experimental investigation of rotational resistance of a spiral-type robotic capsule inside a real intestine. *IEEE-ASME Transactions on Mechatronics*, 18 (5), 1555-1562.

Modeling and Experimental Investigation of Rotational Resistance of a Spiral-Type Robotic Capsule Inside a Real Intestine

Hao Zhou, Gursel Alici, Trung Duc Than, and Weihua Li

Abstract—In this study, the rotational resistance of a spiral-type capsule rotating inside a small intestine is investigated by *in vitro* experiments and analytical modeling, on which a limited literature is available. The results presented exhibit viscoelastic nature of the intestinal tissue. The significance of various spiral structures and rotating speeds is quantitatively evaluated from the propulsion point of view. Also, an analytical torque model is proposed and subsequently validated. The close match between the experimental results and numerical results from the model shows that the model is reasonably accurate to estimate the rotational resistance torque of the small intestine. Both the experimental and modeling works provide a useful guide to determine the torque required for a spiral-type endoscopic capsule operating in a “really” small intestine. Therefore, the proposed torque model can be used in the design and optimization of in-body robotic systems, which can remotely be articulated using magnetic actuation.

Index Terms—

I. INTRODUCTION

THE wireless capsule endoscope (WCE) has been universally used as a first-line medical tool to diagnose diseases in the gastrointestinal (GI) tract, especially in the small intestine, where traditional endoscopes are hard to access [1]–[3]. It is believed that more attractive applications of WCE, such as targeted drug delivery and telepresence surgery, will be realized in the near future if a robotic capsule with active locomotion is developed to break its dependence on the natural peristalsis for movement [4].

Significant effort has been dedicated to exploring novel locomotion mechanisms [5]–[8]. Among them, magnetic propulsion is promising since it does not require onboard batteries and the control unit is moved out of the capsule, too. Therefore, much space can be saved, which is a vital advantage for a millisized robotic device or even smaller size. In addition, a limited opera-

tion time will no longer be a problem due to remotely powering of a magnetically propelled robotic device.

Two approaches are generally adopted to implement magnetic propulsion. The first approach [9]–[11] is straightforward, exerting a direct pulling force on an internal magnetic part by producing a magnetic field gradient. However, this pulling force decays rapidly when the gap between the robot and the magnetic source increases. The second approach [12], [13] is based on embedding a magnet with its magnetization lateral to the capsule’s axis and then generating a rotating magnetic field so that the capsule can be acted upon by a magnetic torque and hence the capsule spins about its axis. When a spiral structure is mounted on the capsule’s surface, the rotation is converted to a translational movement. Compared to the direct-pulling method, the propulsion of a spiral-type robot is advantageous because the maximum torque available to the robot is proportional to the magnetic field intensity, which declines slower than the magnetic field gradient over a long distance. Three-axis Helmholtz coils with three separate sinusoidal current inputs are able to produce a rotating magnetic field with a uniform intensity and an adjustable rotational axis so that the robot is propelled and steered along the curved GI tract [13].

To develop a spiral-type WCE, the geometry of the helical structure must be optimized since it plays a significant role in determining the propulsion efficiency. As a medical micro-robot traveling in a deflated, winding, and slippery lumen, the complexity of its working environment makes this optimization problem even more critical. Therefore, the resistant characteristics of the GI tract should be evaluated in order to provide more accurate data with the optimization process.

Recently, some research work has been reported on the biomechanical and tribological properties of the GI tract. Baek *et al.* measured the frictional resistance of capsules with different shapes and dimensions moving along porcine small intestinal samples and concluded that a smooth cylindrical capsule with a smaller diameter performed better in avoiding translational friction [14]. In their work, they investigated the small intestine’s properties further and reported on a viscoelasticity model for the stress relaxation [15] as well as an analytical model [16] to predict the friction from a linear movement of a smooth cylindrical capsule inside the small intestine. Wang and Meng conducted a series of tests with 15 plastic capsules of various diameters and lengths inside the segments of porcine small intestine [17]. The resistant forces from 20 to 100 mN were measured for the capsules which had the diameters in the range of 8–13 mm and the translational speed of 0.5 mm/s. Wang and Yan performed

Manuscript received January 4, 2012; revised April 16, 2012; accepted July 2, 2012. Recommended by Technical Editor Y. Sun. This work was supported by the Intelligent Nano-Tera Systems Research Laboratory of the University of Wollongong. The work of H. Zhou and T. D. Than was supported by the University of Wollongong Research Council under the Ph.D. scholarships.

The authors are with the School of Mechanical, Materials and Mechatronic Engineering, University of Wollongong, Wollongong, N.S.W., 2522, Australia (e-mail: hz467@uowmail.edu.au; gursel@uow.edu.au; dtt581@uowmail.edu.au; weihuali@uow.edu.au).

Color versions of one or more of the figures in this paper are available online at <http://ieeexplore.ieee.org>.

Digital Object Identifier 10.1109/TMECH.2012.2208121

84 the tests by pulling a set of specially prepared frictional samples
 85 with different surface profiles on planar open intestinal sam-
 86 ples [18]. The tests showed that a flat contact surface caused
 87 the least resistance while a triangular one led to the most. Terry
 88 *et al.* performed experiments on active forces from the myen-
 89 teron, biomechanical response, mucus adhesivity, and tribology
 90 of the porcine small intestine [19]. By comparing the *in vivo* and
 91 *in vitro* tribometry tests, it was suggested that the coefficient of
 92 friction (COF) might slightly drop as the tissue became dead.
 93 Bellini *et al.* proposed a constitutive model, with parameters
 94 identified from planar biaxial test data, to predict biomechan-
 95 ical response of the small bowel under complex loading [20].
 96 All these work has contributed to a better understanding of
 97 the mechanical properties of the small intestine for active cap-
 98 sule endoscopes. However, none of them studied the frictional
 99 resistance for a spiral-type capsule rotating inside a small intes-
 100 tine, which represents the real operation condition of a robotic
 101 capsule. This study aims to close this gap in the literature by
 102 establishing a mathematical model to predict the mechanical
 103 torque required to rotate the robotic capsule in a viscoelastic
 104 environment such as the GI tract.

105 This paper investigates the rotational resistance of a spiral-
 106 type capsule rotating inside the GI tract. From a physiological
 107 point of view, this is the resistance which the robotic capsule
 108 must overcome in order to start and maintain its rotation. The
 109 small intestine of a porcine was employed for the *in vitro* exper-
 110 iments since its mechanical properties were reported to be quite
 111 similar to those of a human being [21]. Four capsules with differ-
 112 ent spiral structures were tested under various rotating speeds.
 113 The rotational resistance was measured and presented in the
 114 form of torque. Furthermore, an analytical model was proposed
 115 for the prediction of this frictional resistance. Some paramet-
 116 ers were identified with one set of experimental results and
 117 other sets of experimental results were used to further validate
 118 the model. This study provides a useful guide to characterize
 119 the required torque for a spiral-type capsule and to undertake the
 120 design and optimization of the microrobots' traction topology.

121 II. EXPERIMENTS

122 A. Experimental Setup

123 Dummy Pillcam SB2 capsules (Given Imaging) were adopted
 124 as the bases of the microrobots. For each capsule, a segment
 125 of wire (ϕ 1 mm) was wound around the outer surface and
 126 acted as the spiral structure. The winding area was within the
 127 cylindrical part of the capsule so that every spiral structure
 128 had the same dimension (15 mm) in the longitudinal axis. Four
 129 spiral-type capsules of such were fabricated, with the helical
 130 angles of 5° (No. 1), 10° (No. 2), 15° (No. 3), and 20° (No. 4),
 131 respectively, as shown in Fig. 1. For each of them, only one
 132 spiral was attached on the surface.

133 A steel rod was fixed to one end of the capsule so that the
 134 assembly could be connected to a torque sensor, which was able
 135 to output real-time measurements to its indicator. Via an RS232
 136 cable and an interface program, the data were consequently sent
 137 to a PC for recording. During the tests, the capsule was kept still
 138 and the small intestine was spinning instead. The segment was



Fig. 1. Capsules with different spiral structures.

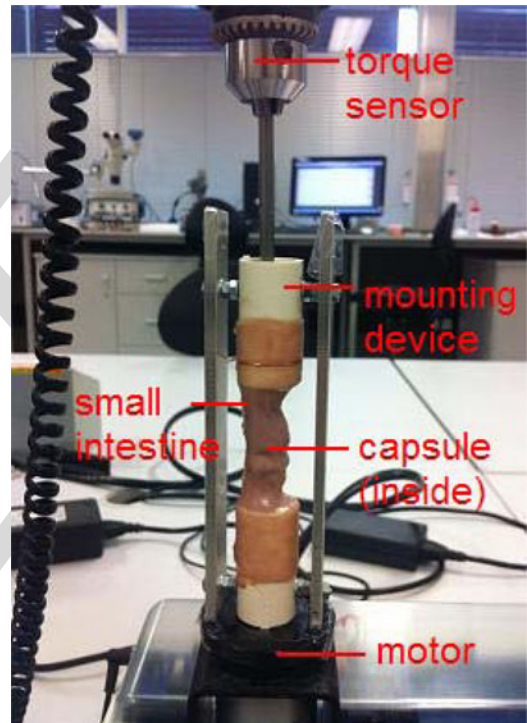


Fig. 2. General view of the experimental setup.

139 mounted on a custom-built device, comprised of two coaxial
 140 plastic tubes and two aluminum bars for supporting. Then, this
 141 device was attached to an electric motor, whose rotating speed
 142 was adjusted by a Labview program sending commands via a
 143 data-acquisition (DAQ) board and a control module. In order
 144 to avoid the influence from the gravity, the devices were lined
 145 up vertically. The general view of the experimental setup is
 146 illustrated in Fig. 2.

147 B. Experimental Procedures

148 The intestinal specimens, kept in a refrigerator, were unfrozen
 149 a few hours before the experiments. Then, they were immersed
 150 in a jar of physiological saline, which was helpful to prevent tis-
 151 sue rupture. One intestinal segment and one capsule were placed
 152 as shown in Fig. 2 each time. The small intestine was rotated
 153 at a constant speed for several seconds by the electric motor
 154 so that the real-time frictional torque could be measured by the
 155 torque sensor. An initial test was carried out with one specimen

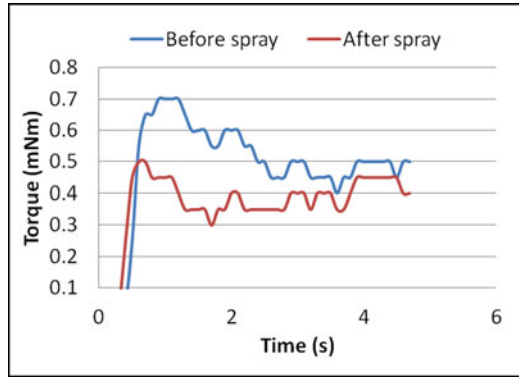


Fig. 3. Initial test with the small intestine Sample 1.

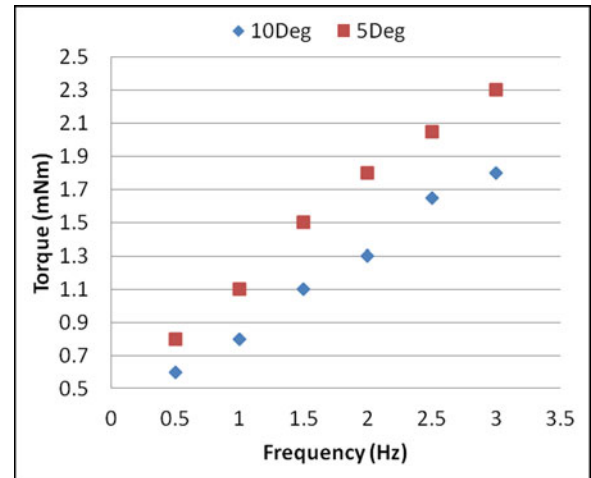


Fig. 4. Torque Measurement with the small intestine Sample 2.

156 (Sample 1). Afterward, a set of tests were performed with the
 157 other two intestinal specimens successively. The internal diam-
 158 eters were 10.9 mm (Sample 2) and 11.1 mm (Sample 3),
 159 respectively. Both of them had the thickness of 1 mm. For each
 160 set of test, the rotating frequencies in the range of 0.5–3 Hz were
 161 applied.

162 The small intestine would be dried out fast once it was dis-
 163 placed out of the fluid. However, the saline could not be sprayed
 164 on the segment during the experiment since it would change
 165 the frictional properties of the intestine, as explained in the fol-
 166 lowing section. Therefore, in order to keep the experimental
 167 conditions as consistent as possible, the tests were finished in a
 168 short time for either Sample 2 or Sample 3. Additionally, after
 169 each measurement, the sample was inspected whether a slight
 170 twist occurred due to the contact with the capsule. If so, a quick
 171 and simple treatment would be conducted manually to bring it
 172 back to the original state.

173 When all the tests for one specimen were finished, the in-
 174 testinal tube was cut open and flattened on a table immediately.
 175 By using a force sensor and a smooth capsule with the mass of
 176 3.98 g, the COF was determined for each intestinal specimen by
 177 the following equation:

$$\mu = \frac{f}{m \cdot g} \quad (1)$$

178 where f is the force to overcome the friction, and m is the mass
 179 of the pulled capsule, and g is the gravity of earth.

180 All the experiments were carried out in an air-conditioned
 181 space, which maintained the room temperature at 25 °C.

182 *C. Results and Discussions*

183 Fig. 3 shows the torque measurements with the capsule No. 2
 184 (helical angle = 10°) and the small intestine Sample 1 under
 185 the rotating frequency of 1 Hz. Fig. 4 shows the results with two
 186 different segments. From Fig. 4, a slightly higher static friction
 187 occurs first and then a relatively steady dynamic friction can be
 188 observed. After spraying some saline on Sample 1, a reduction in
 189 the frictional resistance is quite apparent, implying the change of
 190 the tissue’s biomechanical and tribological properties due to the
 191 absorption of liquid. Therefore, humidifying the intestine during

the tests is inappropriate for the consistence of the experimental
 environment.

In the tests with Sample 2 and Sample 3, the measurements
 of dynamic friction are compared to each other as different
 combinations of capsule and intestinal specimens as well as
 frequency were adopted.

Sample 2 was tested with the capsules No. 1 (helical angle =
 5°) and No. 2, respectively. The results are shown in Fig. 4. From
 the graph, it is seen that the frictional torque increases as the
 rotation frequency rises, indicating the rotational resistance has
 a relationship with the rate of strain of the small intestine. This
 dependence reveals the viscoelasticity of the GI tract to some
 extent. Due to the introduction of the spiral, the cross section
 of the capsule in the lateral direction is raised, increasing the
 deformation of the intestine. This increase becomes larger when
 the helical angle gets smaller. Therefore, when the number of
 spiral is the same, a capsule with a smaller helical angle causes
 more strain in the intestine, and consequently, confronts a higher
 frictional resistance. In this case, from 0.5 to 3 Hz, the capsule
 No. 2 (helical angle = 10°) causes a torque in the range of
 0.6–1.8 mN·m while the capsule No. 1 (helical angle = 5°)
 results in the magnitude between 0.8 and 2.3 mN·m. At low
 frequencies, the torque is almost proportional to the frequency
 and the proportionality constant is bigger when the helical angle
 is smaller.

Sample 3 was tested with all the four capsules one by one. The
 torque measurements are presented in Fig. 5. For the same com-
 binations of capsule, specimen, and frequency, the results are
 slightly different from those of Sample 2 due to the discrepancy
 of two intestinal specimens’ conditions. However, the magni-
 tude of the resistant feature is still in the same order. Moreover,
 the trend is nearly identical to that of Sample 2.

The COFs of two intestinal segments were also determined
 by (1) for the parameter identification of the analytical model
 proposed in the following section. Fig. 6 shows a sample mea-
 surement of the force versus time for the smooth capsule to
 overcome the friction on the cut-open and flattened small intes-
 tine (Sample 2). Since the mass of the capsule is already known,

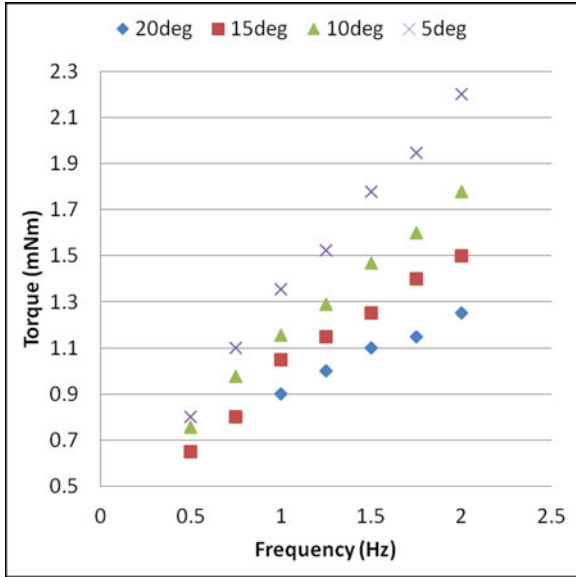


Fig. 5. Torque Measurement with the small intestine Sample 3.

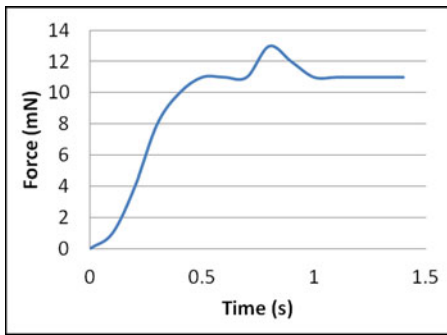


Fig. 6. Force history for a smooth capsule to overcome the friction on the cut-open and flattened small intestine Sample 2.

230 the COF for Sample 2 can be calculated as 0.28. The same
 231 method is used to find the COF for Sample 3, which is equal to
 232 0.51. We postulate that the difference between these COFs can
 233 be due to different wetness conditions on the inner surfaces of
 234 these two samples. The inner surface of Sample 2 was slightly
 235 humidified with the saline before it was tested while the same
 236 treatment was not applied to Sample 3. As reported before,
 237 a small amount of lubrication could change the friction in a small
 238 intestine dramatically [17].

239 III. MODELING

240 A. Viscoelasticity Model

241 Generally, the relationship between stress and strain of a vis-
 242 coelastic material can be illustrated by a generalized Maxwell
 243 model including multiple viscous dashpots and elastic springs
 244 [22]. Fig. 7 shows a five-element linear viscoelastic model,
 245 which is employed to describe the mechanical behavior of the
 246 small intestine in this study. The constitutive equation is ex-

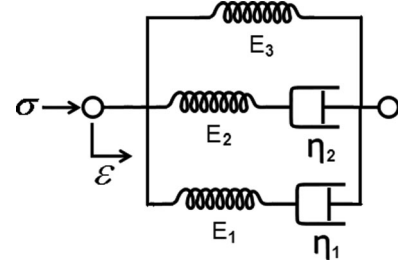


Fig. 7. Five-element viscoelasticity model.

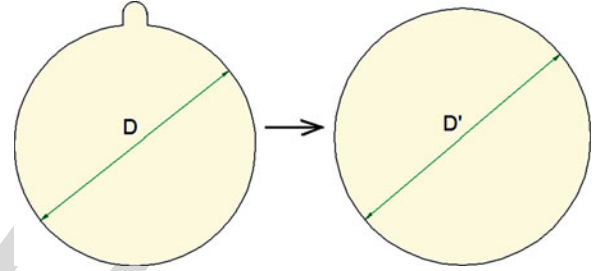


Fig. 8. Conversion of the inner intestinal wall's profile.

pressed as follows:

$$\sigma(t) = \varepsilon(t) \left[E_1 \exp\left(-\frac{tE_1}{\eta_1}\right) + E_2 \exp\left(-\frac{tE_2}{\eta_2}\right) + E_3 \right] \quad (2)$$

247 where σ and ε denote the stress and the strain at the time t ,
 248 respectively, and E_1 , E_2 , and E_3 are the elastic modulus
 249 of springs, and η_1 and η_2 represent the viscosities of dashpots.
 250

251 B. Analytical Model for Rotational Resistance

252 As discussed earlier, attaching a spiral structure on the surface
 253 increases the cross section of the capsule in its lateral direction.
 254 In Fig. 8, the left-hand side profile describes the inner wall's
 255 cross-sectional profile of the small intestine after its deforma-
 256 tion due to the insertion of the spiral-type capsule. The bulge
 257 results from the spiral structure and the parameter D indicates
 258 the diameter of the cylindrical part of Pillcam SB2 capsule
 259 (11 mm). To simplify the analysis, as the capsule rotates, the
 260 contour is converted to a circular geometry whose perimeter is
 261 comparable to the total length of the original one, which means
 262 the circumferential extension of the intestinal tract is kept the
 263 same. The right-hand side profile in Fig. 8 shows the converted
 264 circular profile of the deformed intestine's inner surface with
 265 a new diameter of D' . Since the spiral is only wound on the
 266 cylindrical part, D' is just applied to calculate the strain of tissue
 267 for this area. The practical dimensions are used for the frontal
 268 and rear parts.

269 In addition to this geometrical simplification, a few assump-
 270 tions are made to develop the model.

- 271 1) The intestinal tissue is an isotropic and incompressible
 272 material.
- 273 2) The volume and the wall thickness of the small intestine
 274 are constant.

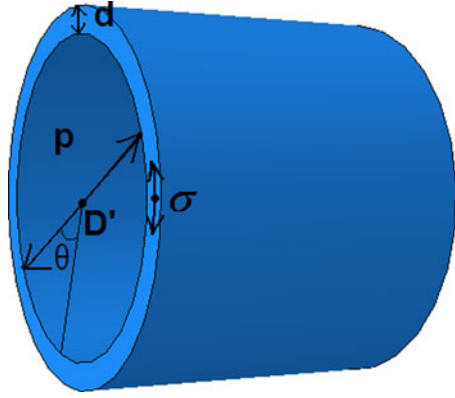


Fig. 9. Pressure vessel for the intestinal tract modeling.

275 3) The deformation of the intestine corresponds to the contact
 276 area and is symmetrical toward the radial direction after
 277 the geometrical simplification.

278 In order to analyze the normal load exerted on the capsule,
 279 the internal pressure generated by the intestinal tract due to
 280 circumferential extension has to be determined. Therefore, the
 281 intestine is modeled as a cylindrical pressure vessel [23] shown
 282 in Fig. 9. The pressure can be calculated from

$$p(\theta) = \frac{\sigma(\theta)2d}{D'} \quad (3)$$

283 where d is the thickness of the small intestine, and D' is the
 284 diameter of the converted inner intestinal surface's profile, and
 285 σ and p are the circumferential stress and the corresponding
 286 pressure at the azimuth θ , respectively.

287 For a rotational movement, the time t is the division of the
 288 azimuth θ by the angular velocity ω . Hence, (2) can be written
 289 to express the relationship between the stress σ and the rotating
 290 frequency f as follows:

$$\sigma(\theta) = \varepsilon(\theta) \left[E_1 \exp\left(-\frac{\theta E_1}{\omega \eta_1}\right) + E_2 \exp\left(-\frac{\theta E_2}{\omega \eta_2}\right) + E_3 \right] \quad (4)$$

$$\omega = 2\pi f. \quad (5)$$

291 For every lateral cross section, the circumferential strain
 292 due to capsule insertion is determined by

$$\varepsilon = \frac{D_{\text{after}} - D_{\text{before}}}{D_{\text{before}} + d} \quad (6)$$

293 where D_{before} and D_{after} are the inner diameters of the intestinal
 294 tract before and after deformation, respectively. For the middle
 295 part with the spiral, D_{after} is equal to D' . For the frontal and
 296 rear parts without the spiral, only the contact areas are taken
 297 into account. Since these parts are semispheres, D_{after} varies
 298 with the axial position and can be calculated with the spherical
 299 radius, which is 5.5 mm.

300 The total normal load for one cross section can be obtained
 301 by using (3) to integrate the pressure along the circumference.
 302 Once the frictional coefficient μ is evaluated, the circumferential
 303 friction can be calculated with Coulomb's law of friction. Since
 304 the distance between the force and rotating axis is fixed, the

 TABLE I
 IDENTIFIED PARAMETERS FOR THE SMALL INTESTINE SAMPLE 2

Parameters	Numerical Values
E_1 (kPa)	0.12
E_2 (kPa)	18.64
E_3 (kPa)	0.0122
η_1 (kPa s)	43.51
η_2 (kPa s)	0.2213

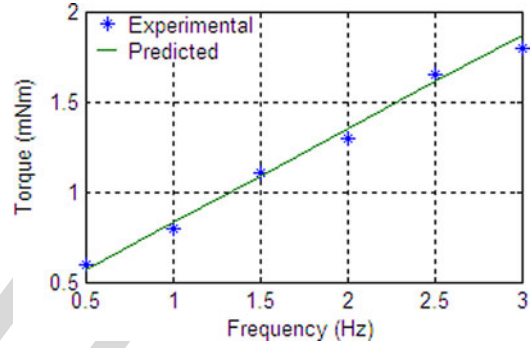


Fig. 10. Variation of the frictional torque with the capsule No. 2 rotating inside the small intestine Sample 2.

rotational resistance can be solved in the form of a resistive
 torque. The equations are expressed as follows:

$$f = \mu \int p(\theta) d\theta \quad (7)$$

$$\tau = \frac{f D_{\text{after}}}{2} \quad (8)$$

where f is the frictional force in the circumferential direction
 and τ is the resistant torque as a result of rotation.

C. Parameter Identification and Model Validation

To identify the elastic modulus and viscosities in the model, a
 nonlinear least square optimization process is employed in this
 study. Based on the nonlinear relationship between the frictional
 torque and the rotating frequency, these material parameters
 were estimated by means of minimizing the summed square of
 the error vector with the experimental data presented earlier. A
 numerical search method, which is the interior-reflective New-
 ton algorithm, was used to solve the problem. It acquires the
 approximate solution of a system by utilizing the method of
 preconditioned conjugate gradients at each iteration. It is sug-
 gested that this method is efficient for nonlinear optimization
 problems [24].

For the small intestine Sample 2, the measurements with the
 capsule No. 2 (helical angle = 10°) was used to estimate the
 parameters. The numerical values are listed in Table I. The
 experimental and predicted frictional torques corresponding to
 the frequencies are shown in Fig. 10.

The measurements with the capsule No. 1 (helical angle = 5°)
 was used to validate the model for the small intestine Sample 2
 shown in Fig. 11. With reference to these results, the estimated
 values are quite consistent to the experimental results, indicat-
 ing that the analytical model is effective enough to predict the

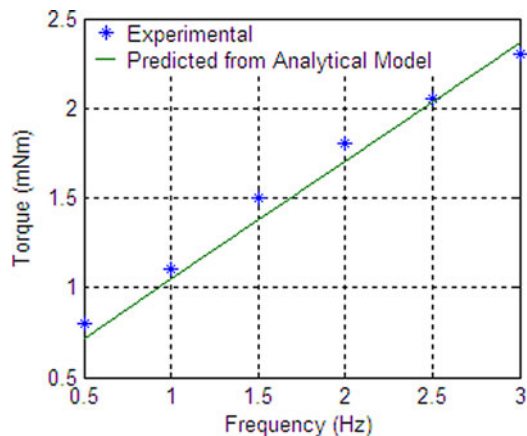


Fig. 11. Validation for the small intestine Sample 2.

TABLE II
IDENTIFIED PARAMETERS FOR THE SMALL INTESTINE SAMPLE 3

Parameters	Numerical Values
E_1 (kPa)	0.0348
E_2 (kPa)	0.7722
E_3 (kPa)	0.0448
η_1 (kPa s)	9.491
η_2 (kPa s)	0.2489

332 rotational resistance resulting from the spiral-type capsule ro-
333 rotating inside the small intestine Sample 2.

334 Though the trend of mechanical behavior is identical, the spec-
335 ific viscoelasticity of the intestinal tract may be different from
336 one sample to another due to many experimental factors such as
337 the freezing period, humidification level, and even variation in
338 the tissue's microstructure. Therefore, the nonlinear least square
339 optimization was repeated to identify the elastic modulus and
340 viscosities of the model for the small intestine Sample 3. The
341 measurements with the capsule No. 3 (helical angle = 15°) was
342 employed. The estimated parameters are listed in Table II. The
343 experimental and predicted resistant torque values are presented
344 in Fig. 12. These results also demonstrate the efficacy of the an-
345 alytical model in predicting the mechanical torque needed to
346 overcome resistive effects associated with the viscoelastic in-
347 testine environment.

348 To evaluate the accuracy of the model for Sample 3, the
349 measurements with other three capsules were compared to the
350 predicted values with the estimated parameters, as illustrated
351 in Fig. 13. With reference to these results, the model performs
352 well when predicting the rotational resistance (i.e., torque) of
353 the capsule No. 2 (helical angle = 10°). Though the prediction's
354 accuracy is a bit lower for the other two capsules, the prediction
355 is still in a reasonable range. We postulate that the discrepancy is
356 possibly due to the effect of the stress concentration around the
357 spiral structure, which is neglected in this model. In addition,
358 the condition of the small intestine Sample 3 might slightly
359 change during the tests due to a relatively longer experimental
360 time compared to that with Sample 2.

361 From the estimated parameters for Sample 2 and Sample 3, it
362 can be seen that the mechanical properties of different segments

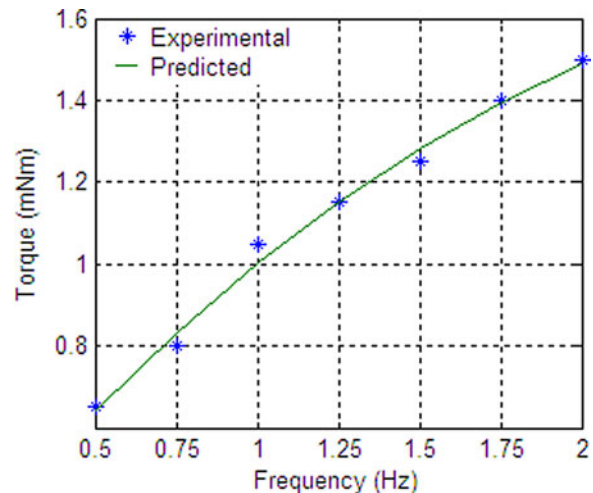


Fig. 12. Variation of the frictional torque with the capsule No. 3 rotating inside the small intestine Sample 3.

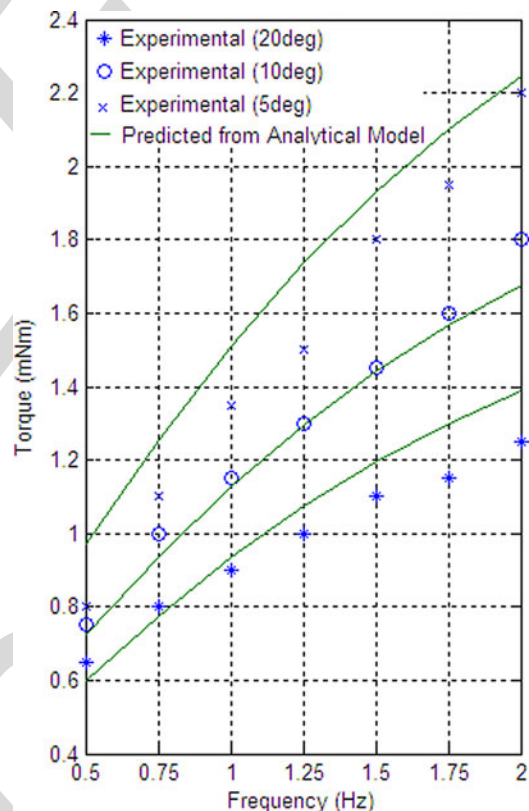


Fig. 13. Validation for the small intestine Sample 3.

(i.e., samples) exhibit some variance as expected, though they 363
364 both show the viscoelastic properties and exert the rotational
365 resistance in the same order of magnitude on the inserted capsule
366 due to the deformation and rotation.

IV. CONCLUSION 367

The rotational resistance of a spiral-type capsule rotating in- 368
369 side the small intestine is investigated by both *in vitro* exper-
370 iments and mathematical modeling and analysis, on which a

371 limited literature is available. The experimental results show
 372 the viscoelastic nature of the intestinal tissue and the effects of
 373 various spiral structures and rotating speeds. At low rotating fre-
 374 quencies (0.5–3 Hz), a capsule ($\phi 11 \times 26$ mm) wounded with
 375 a 1-mm-high spiral works against a frictional torque varying
 376 from 0.5 mN·m to several mN·m. The torque increases with the
 377 increase of the frequency. Due to the same number of spiral in
 378 the tests, the helical structure with a smaller helical angle raises
 379 more in the lateral cross section of the robotic capsule, which
 380 results in more circumferential deformation of the small intestine
 381 and more rotational resistance. Viscoelastic properties of
 382 the “real” intestine are identified using a nonlinear optimization
 383 method. The validation results show that the proposed torque
 384 model is reasonably effective to estimate the rotational resistive
 385 torque of the small intestine. For different intestinal samples,
 386 though the rotational resistance is in the same order of magni-
 387 tude, their biomechanical and tribological properties may show
 388 some variance due to the different conditions such as the du-
 389 ration of freezing time, intestine size, capsule weight, and hu-
 390 midification level. Both the experimental and modeling work
 391 provide a useful reference to characterize the required torque
 392 for a spiral-type capsule and, therefore, helps to undertake the
 393 design and optimization of the microrobots for medical use in
 394 the GI tract. However, before such a spiral-type robot is used
 395 in a real GI tract, *in vivo* experiments should be conducted in
 396 a highly unstructured, slippery, deformable, and nonsmooth en-
 397 vironment to obtain a more accurate estimate of the rotational
 398 resistance.

399 Further work will aim to conduct more experiments with vari-
 400 ous intestinal specimens and improve the analytical model so
 401 that the stress concentration and viscoelastic properties due to
 402 variable-size spiral structures can be taken into account. Further-
 403 more, some addition will be made to the current experimental
 404 setup so that a rotational and translational movement can be
 405 allowed between the capsule and the inner wall of the small
 406 intestine. The rotational resistance with different translational
 407 speed of the capsule will be investigated and compared to the
 408 current results.

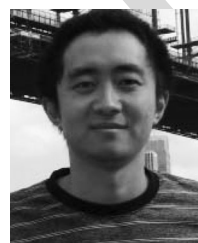
ACKNOWLEDGMENT

409 The authors would like to thank Given Imaging Pty. Ltd,
 410 Sydney, Australia, for providing the endoscopic capsules used
 411 in this study.
 412

REFERENCES

- 414 [1] R. Eliakim, “Video capsule endoscopy of the small bowel,” *Curr. Opin.*
 415 *Gastroenterol.*, vol. 26, pp. 129–133, 2010.
 416 [2] M. Waterman and R. Eliakim, “Capsule enteroscopy of the small intestine,”
 417 *Abdominal Imag.*, vol. 34, pp. 452–458, 2009.
 418 [3] H. Niemenmaa, T. Mäkelä, A. Jussilia, I. Krekelä, M. Voutilainen,
 419 H. Björknäs, A. Hirvioja, K. Kaukinen, and P. Collin, “The diagnos-
 420 tic value of video capsule endoscopy,” *Eur. J. Internal Med.*, vol. 21,
 421 pp. 383–385, 2010.
 422 [4] A. Moglia, A. Menciassi, P. Dario, and A. Cuschieri, “Capsule endoscopy:
 423 Progress update and challenges ahead,” *Nat. Rev. Gastroenterol. Hepatol.*,
 424 vol. 6, pp. 353–362, 2009.
 425 [5] A. Moglia, A. Menciassi, and P. Dario, “Recent patents on wireless capsule
 426 endoscopy,” *Recent Patents Biomed. Eng.*, vol. 1, pp. 24–33, 2008.

- [6] J. L. Toennies, G. Tortora, M. Simi, P. Valdastrì, and R. J. Webster III, “Swallowable medical devices for diagnosis and surgery: The state of the art,” *Proc. IMech C, J. Mech. Eng. Sci.*, vol. 224, pp. 1397–1414, 2010.
 [7] B. Kim, S. Lee, J. H. Park, and J. O. Park, “Design and fabrication of a locomotive mechanism for capsule-type endoscopes using shape memory alloys (SMAs),” *IEEE/ASME Trans. Mechatronics*, vol. 10, no. 1, pp. 77–86, Feb. 2005.
 [8] M. Simi, P. Valdastrì, C. Quaglia, A. Menciassi, and P. Dario, “Design, fabrication, and testing a capsule with hybrid locomotion for gastrointestinal tract exploration,” *IEEE/ASME Trans. Mechatronics*, vol. 15, no. 2, pp. 170–180, Apr. 2010.
 [9] F. Carpi, N. Kastelein, M. Talcott, and C. Pappone, “Magnetically controllable gastrointestinal steering of video capsules,” *IEEE Trans. Biomed. Eng.*, vol. 58, no. 2, pp. 231–234, Feb. 2011.
 [10] F. Carpi, “Magnetic capsule endoscopy: The future is around the corner,” *Expert Rev. Med. Devices*, vol. 7, pp. 161–164, 2010.
 [11] M. Gao, C. Hu, Z. Chen, H. Zhang, and S. Liu, “Design and fabrication of a magnetic propulsion system for self-propelled capsule endoscope,” *IEEE Trans. Biomed. Eng.*, vol. 57, no. 12, pp. 2891–2902, Dec. 2010.
 [12] M. Sendoh, K. A. Yamazaki, A. Chiba, M. Soma, K. Ishiyama, and K. I. Arai, “Spiral type magnetic micro actuators for medical applications,” in *Proc. Int. Symp. Micro-NanoMechatronics. Human Sci.*, 2004, pp. 319–324.
 [13] Y. Zhang, S. Jiang, X. Zhang, X. Ruan, and D. Guo, “A variable-diameter capsule robot based on multiple wedge effects,” *IEEE/ASME Trans. Mechatronics*, vol. 16, no. 2, pp. 241–254, Apr. 2011.
 [14] N. K. Baek, I. H. Sung, and D. E. Kim, “Frictional resistance characteristics of a capsule inside the intestine for microendoscope design,” *Proc. Instn Mech. Eng. J, Eng. Med.*, vol. 218, pp. 193–201, 2004.
 [15] J. S. Kim, I. H. Sung, Y. T. Kim, E. Y. Kwon, D. E. Kim, and Y. H. Jang, “Experimental investigation of frictional and viscoelastic properties of intestine for microendoscope application,” *Tribol. Lett.*, vol. 22, pp. 143–149, 2006.
 [16] J. S. Kim, I. H. Sung, Y. T. Kim, and Y. H. Jang, “Analytical model development for the prediction of the frictional resistance of a capsule endoscope inside an intestine,” *Proc. Instn Mech. Engrs PartH: J. Eng. Med.*, vol. 221, pp. 837–845, 2007.
 [17] X. Wang and M. Q. H. Meng, “An experimental study of resistant properties of the small intestine for an active capsule endoscope,” *Proc. Instn Mech. Engrs PartH: J. Eng. Med.*, vol. 224, pp. 107–118, 2010.
 [18] K. D. Wang and G. Z. Yan, “Research on measurement and modeling of the gastro intestine’s frictional characteristics,” *Meas. Sci. Technol.*, vol. 20, p. 015803 (6pp), 2009.
 [19] B. S. Terry, A. B. Lyle, J. A. Schoen, and M. E. Rentschler, “Preliminary mechanical characterization of the small bowel for *in vivo* robotic mobility,” *ASME J. Biomech. Eng.*, vol. 133, pp. 091010-1–091010-7, 2011.
 [20] C. Bellini, P. Glass, M. Sitti, and E. S. Di Martino, “Biaxial mechanical modeling of the small intestine,” *J. Mech. Behav. Biomed. Mater.*, vol. 4, pp. 1727–1740, 2011.
 [21] H. D. Hoeg, A. B. Slatkin, and J. W. Burdick, “Biomedical modeling of the small intestine as required for the design and operation of a robotic endoscope,” in *Proc. IEEE Int. Conf. Rob. Autom.*, 2000, pp. 1599–1606.
 [22] W. Flugge, *Viscoelasticity*. Berlin, Germany: Springer-Verlag, 1975.
 [23] J. M. Gere, *Mechanics of Materials*, 7th ed. Toronto, ON, Canada: Cengage Learning, 2009.
 [24] G. Alici, “An effective modeling approach to estimate nonlinear bending behavior of cantilever type conducting polymer actuators,” *Sens. Actuators B, Chem.*, vol. 141, pp. 284–292, 2009.



Hao Zhou received the B.S. degree in building environment and facility engineering from Tongji University, Shanghai, China, in 2004, the M.S. degree in mechanical engineering from the University of Queensland, Australia, in 2008, and the M.S. degree in engineering practice (mechanical) from the University of Wollongong, Wollongong, Australia, in 2009, where he is currently working toward the Ph.D. degree.

His research interests include simulations and analysis of electromagnetics, simulations and analysis of biomechanics of the small intestine, mechanics of viscoelastic materials, and active locomotion of wireless capsule endoscopy.

500
501
502
503
504
505
506
507
508
509
510
511
512
513
514
515
516
517
518
519



Gursel Alici received the Ph.D. degree in robotics from the Department of Engineering Science, Oxford University, Oxford, U.K., in 1994.

He is currently a Professor at the University of Wollongong, Wollongong, Australia, where he is the Head of the School of Mechanical, Materials and Mechatronic Engineering. His current research interests include intelligent mechatronic systems involving mechanisms/serial/parallel robot manipulators, micro/nano robotic systems for medical applications, and modeling, analysis, characterization, and control of conducting polymers as macro/micro/nanosized actuators and sensors for robotic and bioinspired applications. He has produced more than 200 refereed publications in his areas of research.

Dr. Alici was a Technical Editor of the IEEE/ASME TRANSACTIONS ON MECHATRONICS during 2008–2012, and is a member of the Mechatronics National Panel formed by the Institution of Engineers, Australia. He was the recipient of the Outstanding Contributions to Teaching and Learning Award from the University of Wollongong, in 2010.

520
521
522
523
524
525
526
527
528
529
530
531



Trung Duc Than received the B.S. degree in electrical engineering from the Hanoi University of Technology, Hanoi, Vietnam, in 2007, and the M.S. degree in electrical and computer engineering from the University of Wollongong, Wollongong, N.S.W., Australia, in 2010, where he is currently working toward the Ph.D. degree in the School of Mechanical, Materials, and Mechatronic Engineering.

His research interest includes the development of localization and control systems for robotic applications.



Weihua Li received the B.Eng. degree in 1992 and the M.Eng. degree in 1995 both from the University of Science and Technology of China and the Ph.D. degree from Nanyang Technological University (NTU), Singapore, in 2001.

After two year's postdoctoral training at NTU, he joined the University of Wollongong, Wollongong, Australia, as a Full-Time Academic, where he is currently working as a Discipline Advisor for Mechatronic Engineering. He has multidisciplinary areas of expertise, including smart materials and structures, microfluidics, intelligent mechatronics, and dynamics and vibration control. He has coauthored more than 160 articles, and delivered many plenary or invited talks at various international conferences.

Dr. Li is currently serving as an Editorial Board member for more than eight international journals.

532
533
534
535
536
537
538
539
540
541
542
543
544
545
546
547
548

IEEE
Proof

QUERIES

549

- Q1: Author: Please supply index terms/keywords for your paper. To download the IEEE Taxonomy go to http://iee.org/documents/2009Taxonomy_v101.pdf. 550
551
- Q2: Author: Please verify the affiliation as set. 552
- Q3. Author: Please provide the full page range in reference [18]. 553

IEEE
Proof